

## CHAPTER 3

### Experimental Procedure

In this chapter, the details of experimental processes are described: chemical reagent and equipment, synthetic procedure and characterization methods are completely illustrated their information as follows.

#### 3.1 Chemical reagents and equipment

##### 3.1.1 Chemical reagents

- 1) Ammonium Molybdate,  $(\text{NH}_4)_6\text{Mo}_7\text{O}_{24}\cdot 4\text{H}_2\text{O}$ , 99.0%, Guangdong, China
- 2) Copper powder (Cu), 99.0%, Riedel-De Haen, Germany
- 3) Silver paint, high purity, SPI supplies, U.S.A.

##### 3.1.2 Equipment

- 1) Analytical balance, model BP-210S, Sartorius AG, Germany
- 2) Microwave oven, model 2820S, Electrolux
- 3) Scanning Electron Microscope and Energy Dispersive X-ray Spectroscopy, model JEM-6335, JEOL, Japan
- 4) Transmission Electron Microscope, model JEM-2010, JEOL, Japan
- 5) X-ray Diffractometer, model D500, SIEMENS, Germany

- 6) Raman spectroscopy, model T64000 JY, Horiba JobinYvon, France
- 7) Luminescence spectrometer, model LS50B, Perkin Elmer, USA
- 8) Fourier transform infrared spectrometer, Model Tensor 27, Bruker, USA
- 9) System source meter, model 2611A, Keithley, U.S.A.
- 10) High DC current power supply, model Welarc 200, Welpro, Thailand
- 11) X-ray photoelectron spectrometer, model AXIS ULTRADLD, Kratos analytical, UK.
- 11) Flow rate controller, model PMR1-010333, Cole-Parmer, U.S.A.

## **3.2 Experimental procedure**

### **3.2.1 MoO<sub>3</sub> : Synthesis using plasma microwave method and optical characterization**

- 1) Synthesis of MoO<sub>3</sub>

To produce MoO<sub>3</sub>, (NH<sub>4</sub>)<sub>6</sub>Mo<sub>7</sub>O<sub>24</sub>·4H<sub>2</sub>O powder was used as a starting material without further purification. Each 0.5 g powder was loaded into three 14-mm-I.D. x 100-mm-long silica boats. Each was placed in a horizontal quartz tube (Figure 3.1), which was tightly closed and evacuated until its absolute pressure was  $3.7 \pm 0.1$  kPa. The powder was heated in batches by a 900 W microwave plasma and each batch was irradiated for 5 min. After the processing of each batch, the powder was thoroughly mixed and repeatedly heated for a total of 40, 50 and 60 min. During processing, the horizontal quartz

tube was continuously evacuated to drain the evolved gases out of the system.

## 2) Characterization

The products were characterized using an X-ray diffractometer (XRD) operating at 20 kV, 15 mA, and using Cu-K $\alpha$  line, in combination with the database of the Joint Committee on Powder Diffraction Standards (JCPDS) [111]; scanning electron microscope (SEM) operating at 15 kV; transmission electron microscope (TEM), and selected area electron diffractometer (SAED) operating at 200 kV; Fourier transform infrared spectrometer (FTIR) with KBr as a diluting agent and operated in the range of 2000-400 cm $^{-1}$ ; Raman spectrometer using a 50 mW and 514.5 nm wavelength Ar green laser; and photoluminescence (PL) spectrometer using a 380 nm excitation wavelength at room temperature.

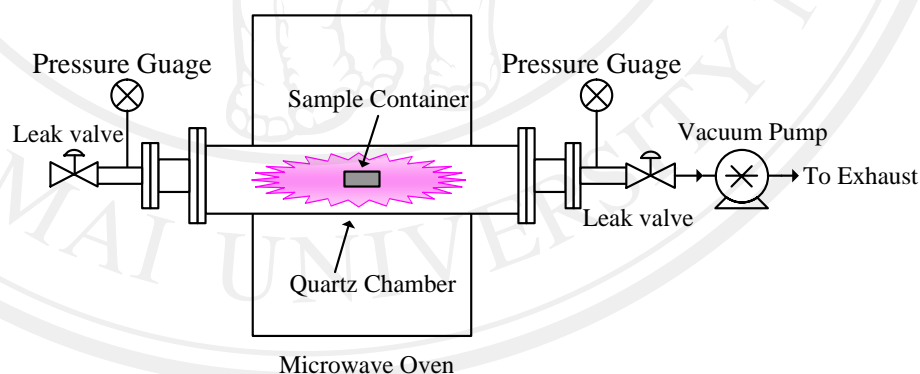


**Figure 3.1** Schematic diagram of microwave induced plasma system.

### 3.2.2 CuO: Synthesis using DC electrical heating method, characterization and gas sensing measurement

#### 1). Synthesis of CuO

Our experiment was carried out by a lab-made DC directly applying voltage (Figure 3.2). Copper powder (99%, Fluka& Riedel-de Haën) was placed between the 2 cm diameter stainless steel electrodes which were connected with DC power supply (Welpro, Welarc 200). To produce copper oxide, the powder was heated by DC electrical supply which directly applied electrical current (50 A, 3.6 V) through the powder for 1, 3, 6, 9, 12 and 15 min in ambient environment. For processing time of longer than 3 min, the powder was heated in batches for 3 min each, left cool down to room temperature, thoroughly mixed at room temperature, and repeatedly heated until reaching the complete processing time.

#### 2). Characterization

Structural and morphological studies were performed by scanning electron microscopy (SEM, JEOL model JSM-6335F) operating at 20 kV and transmission electron microscopy (TEM, JEOL JEM-2010) operating at 200 kV. X-ray diffraction patterns of the samples were recorded on a Rigaku MiniFlexX-ray diffractometer with Cu-K $\alpha$  radiation ( $\lambda = 1.54178 \text{ \AA}$ ). The  $2\theta$  range used in this measurement was from 30 ° to 80 ° in step of 0.02°. The optical properties were characterized using UV-VIS-NIR double beam spectrophotometer (Perkin Elmer, Varian Cary 5000) in the spectral range 200 and 800 nm and photoluminescence (PL) spectrometer (Perkin Elmer, LS50B) with a 325 nm excitation wavelength at room temperature. Fourier transform infrared (FTIR) spectra were recorded on a BRUKER TENSOR 27 Fourier transform

infrared spectrometer with KBr as a diluting agent and operated in the range of 400–4,000  $\text{cm}^{-1}$ . X-ray photoelectron spectroscopy (XPS) model AXIS ULTRA DLD was used to characterize chemical composition of metal oxide surface.

### 3). Fabrication and measurement of sensor

To fabricate a CuO gas sensing device, silver paste was painted on alumina substrates with an interval of 1 mm for using as electrodes, which were solidified by annealing the silver paste at 100 °C for 1 h. The 15 min as-synthesized CuO and DI water were mixed to formulate paste which was used to synthesize films by screen printing. The films were dried at 150 °C for 2 h to remove the binder and to improve the mechanical strength and electrical contact. The measurement of gas sensing properties was studied through a simple static system under normal laboratory condition. The tested gas ( $\text{NH}_3$ ) was calculated the volume before injecting into the air-trapped chamber for controlling the gas concentration. The resistance of sensor was obtained through the electrical current change between those before and after injecting the tested gas to the system (Figure 3.3). The sensitivity (S) can be calculated according to the relation

$$S (\%) = \frac{I_{\text{air}} - I_{\text{gas}}}{I_{\text{air}}} \times 100 \quad (1)$$

where  $I_{\text{air}}$  and  $I_{\text{gas}}$  are the electrical current of the sensor in the surrounding air and tested gas mixture at the same temperature, respectively.

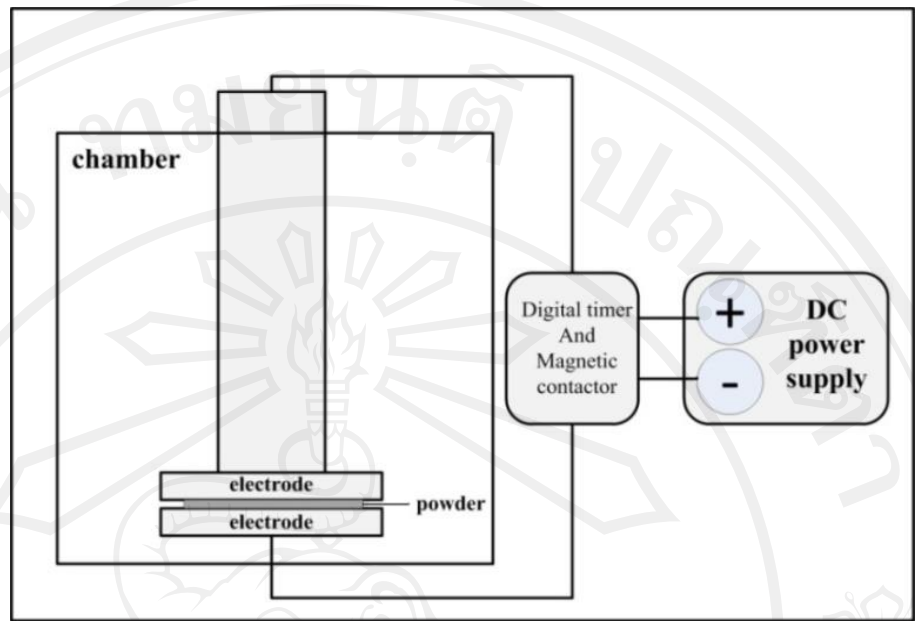


**Figure 3.2** Schematic diagram of a lab-made DC directly applying voltage apparatus.

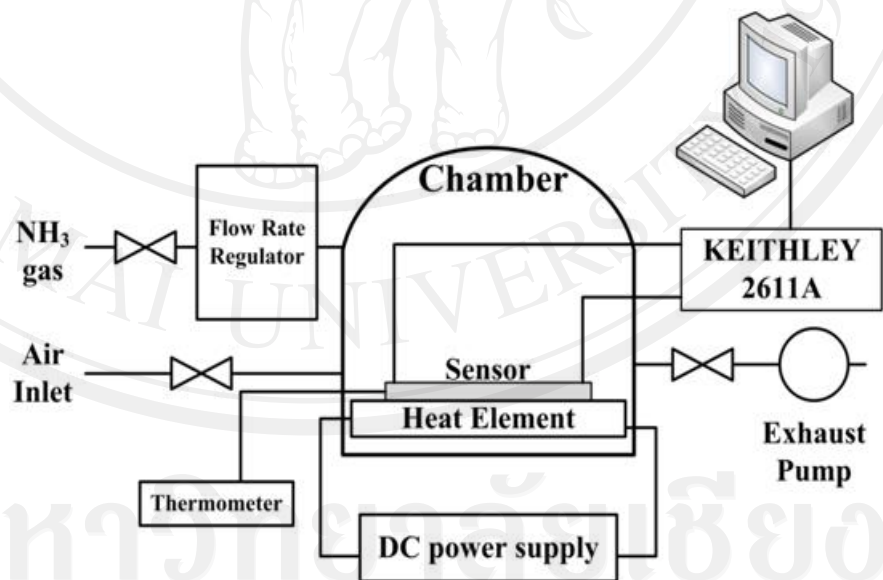


**Figure 3.3** Schematic diagram of a lab-made gas sensing measurement system.



**Figure 3.4** Picture of a lab-made gas sensing measurement system.

### **3.3 Characterization**

#### **3.3.1 X-ray Diffractometer**

The crystallinity and phase purity of the products were analyzed using X-ray diffractometer (XRD, SIEMENS D500, Germany) with Cu K $\alpha$  radiation ( $\lambda = 1.5406 \text{ \AA}$ ) operating at 20 kV 15 mA, at a scanning rate of 0.02 °/s in the  $2\theta$  range of  $10^\circ - 80^\circ$ . The identification of products was analyzed by Philips X'Pert Highscore Computer Software (search-match program) on the database of the Joint Committee on Powder Diffraction Standards (JCPDS)[111].



**Figure 3.5** X-ray diffractometer.

### **3.3.2 Scanning electron microscope**

The morphologies of the samples were determined by a field-emission scanning electron microscope (FESEM) on a JEOL instrument (JSM-6335F) at an accelerating voltage of 15 kV.





**Figure 3.6** Scanning electron microscope.

### **3.3.3 TEM, HRTEM and SAED**

The structures and morphologies of the samples were also characterized from transmission electron microscopy (TEM) images, high-resolution TEM (HRTEM) images and selected area electron diffraction (SAED) patterns. The images were recorded on a JEOL (JEM-2010) transmission electron microscope operate at an acceleration voltage of 200 kV. The preparing method of sample for TEM analysis was to disperse small amount of the as-prepared samples in absolute ethanol, drop this solution onto a copper grid coated with holey carbon film and leave the ethanol to slowly evaporate at room temperature.



**Figure 3.7** Transmission electron microscope.

### **3.3.4 Luminescence spectroscopy**

The luminescence emission spectra of the samples were investigated using Perkin Elmer Luminescence spectrometer LS50B at room temperature.



**Figure 3.8** Luminescence spectrometer.

### 3.3.5 UV-Vis spectroscopy

To investigate optical properties of the products, the UV-vis spectra were measured by UV-vis spectrophotometer (Perkin Elmer, Lambda 19) at room temperature by scanning mode of perkin's software.



**Figure 3.9** UV-VIS spectrophotometer.

### 3.3.6 Raman spectrometer

Raman spectrometer (model T64000, HORIBA Jobin Yvon, U.S.A.) using a 514.5 nm wavelength of Ar green laser with working at 50 mW



**Figure 3.10** Raman spectrometer.

### 3.3.7 Fourier transform infrared spectroscopy

Fourier transform infrared spectroscopy (FTIR, TENSOR 27, BRUKER) with KBr pellet protocol was operated in the range of 400–4000  $\text{cm}^{-1}$ .



**Figure 3.11** Fourier transform infrared spectrometer.

### 3.3.8 System source meter

System source meter was used for apply voltage to gas sensing circuit and measure current at the same time. The I-V characteristic curves can be determined by this meter. The detect output current is at least about  $1 \times 10^{-8}$  A.



**Figure 3.12** System source meter.

### 3.3.9 X-ray photoelectron spectroscopy

The XPS spectrum of sample was investigated by X-ray photoelectron spectrometer (XPS; AXIS ULTRADLD, Kratos analytical, UK.) The pressure in the XPS analyzing chamber was at about  $5 \times 10^{-9}$  torr. The sample was put on the carbon tape which was adhered on a stainless steel plate. Then, the powder was pressed to form a thick film with area about  $3 \times 3$  mm before loading into the X-ray photoelectron spectrometer. The sample was excited by X-ray with spot area of  $700 \times 300$   $\mu\text{m}$  including monochromatic Al  $K\alpha$  1,2 radiation at 1.4 keV. X-ray anode was run at 15 kV 10 mA 150 W. The photoelectrons were detected with a hemispherical analyzer positioned at an angle of  $45^\circ$ .



**Figure 3.13** X-ray photoelectron spectrometer.

### 3.3.10 High DC electrical power supply

For this high DC electrical power supply model, current and power percent output are adjustable. Maximum current output is 200 A. The long time working is available because this machine will be cut off when the circuit is reached at a higher temperature than electrical circuit limit.



**Figure 3.14** High DC electrical power supply.